JOURNAL OF MAGNETIC RESONANCE 78, 292–301 (1988)

Linear Prediction and Projection of Pure Absorption Lineshapes in Two-Dimensional FTESR Correlation Spectroscopy*

JEFF GORCESTER AND JACK H. FREED

Baker Laboratory of Chemistry, Cornell University, Ithaca, New York 14853-1301

Received October 26, 1987; revised November 18, 1987

New ESR experiments based on techniques of two-dimensional correlation spectroscopy have been shown to be useful in the determination of magnetization transfer rates in motionally narrowed nitroxides. Spectral enhancement based upon linear prediction with singular value decomposition (LPSVD) is applied in the present work to project 2D absorption lineshapes and to dramatically improve the signal/noise ratio. Heisenberg spin exchange rates obtained from volume integrals of LPSVD-projected 2D absorption lineshapes compare well with those obtained from absolute value peak amplitudes in the case of 2,2,6,6-tetramethyl-4-piperidone-*N*-oxyl-d_{16} (pd-tempone) dissolved in toluene-d_8 (where theory predicts that the two should agree).

INTRODUCTION

In a recent report we have demonstrated the application of two-dimensional correlation spectroscopy to ESR (*1*). Such techniques are based upon the irradiation of the entire ESR spectrum with a broadband microwave (MW) pulse (*2, 3*) and the recording of the free precession signal (i.e., free induction decay or FID) that follows. More recently we have demonstrated the quantitative capability of ESR correlation spectroscopy with a three-pulse experiment (2D ELDOR) for the observation of magnetization transfer between hyperfine (hf) lines (*4*). In (*4*) we determined the rate of Heisenberg exchange by comparison of peak heights in the absolute value representation of the 2D ELDOR spectrum. The theory indicates, however, that it is the volume integrals of the 2D absorption lines, not the absolute value peak heights, which correctly reflect the electron spin population differences in the general case. In (*4*) we depended on the fact that ratios of absolute value peak heights give the same information as ratios of 2D absorption volume integrals when T_2 is the same for each hf line. In general there is significant variation of T_2 across the spectrum, in which case volume integrals of the 2D absorption lines are essential for accurate measurement of magnetization transfer rates.

The ESR spectrum obtained upon Fourier transformation of the FID is, in general, an admixture of absorption and dispersion. In order to obtain the pure absorption spectrum, numerical phase corrections are required (*3*). The phase of each resonance line depends on the resonance offset of that line as well as on the dead time of the spectrometer (*4*). We observe an almost linear variation of the phase of the recorded signal on frequency (*5*). During the spectrometer dead time, a component of the free

* Supported by NIH Grant GM-25862 and NSF Grant CHE 8703014.

0022-2364/88 $3.00

precession signal may undergo several periods of oscillation, leading to a phase shift of as much as 6π radians for a resonance offset of 50 MHz. For a spectrum of bandwidth 100 MHz, this implies a total phase variation of 12π radians across the spectrum. Numerical correction of this phase variation is accomplished by a simple coordinate transformation in the frequency domain of the real and imaginary outputs of the FFT. Given a complex spectral function $S(\nu)$, the expression for this coordinate transformation is

$$\begin{bmatrix} \mathrm{Re}[S(\nu)] \\ \mathrm{Im}[S(\nu)] \end{bmatrix} = \begin{bmatrix} \cos\alpha & \sin\alpha \\ -\sin\alpha & \cos\alpha \end{bmatrix} \begin{bmatrix} \mathrm{Re}[S(\nu)]' \\ \mathrm{Im}[S(\nu)]' \end{bmatrix}, \qquad [1]$$

where α consists of a frequency-independent correction (the so-called zeroth-order correction) and a frequency-dependent correction (a first-order or linear correction), i.e., $\alpha = \alpha_0 + \alpha_1\nu$. Such corrections are feasible in one-dimensional FTESR (*3*), but are very cumbersome when applied in both dimensions of a two-dimensional spectrum because of the large required linear corrections.

Two-dimensional correlation spectroscopy ("COSY") in ESR is performed in much the same way as for NMR. The pulse sequence $\pi/2$–t_1–$\pi/2$–t_2 constitutes the simplest of the COSY experiments. The initial $\pi/2$ pulse generates the transverse magnetization components which precess during the evolution period t_1 becoming amplitude encoded according to their precessional frequencies in the rotating frame. The FID is recorded during the detection period of duration t_2, which begins with the final $\pi/2$ pulse. The closely related experiment, 2D ELDOR, uses three MW pulses in the sequence $\pi/2$–t_1–$\pi/2$–T–$\pi/2$–t_2. Magnetization transfer is revealed by cross correlations which give rise to 2D ELDOR cross peaks. Peaks which appear along the diagonal in 2D COSY type experiments are associated with autocorrelations and are thus called auto peaks. In each type of 2D experiment an FID is collected for each t_1; then the phase of the first pulse is advanced by 90°, and a second FID is collected [call them $s'(t_1, t_2)$ and $s''(t_1, t_2)$]. These two signals depend on terms oscillatory in t_1 that are in phase quadrature (*6*). Fourier transformation with respect to t_2 of each data set yields the spectral functions $\hat{s}'(t_1, \omega_2)$ and $\hat{s}''(t_1, \omega_2)$. Baseplane corrections facilitate suppression of axial peaks (*4*) after which we form

$$\hat{s}(t_1, \omega_2) = \mathrm{Re}[\hat{s}'] + i\,\mathrm{Re}[\hat{s}''] \qquad [2]$$

which yields the 2D spectrum $S(\omega_1, \omega_2)$ upon final FT.

This two-step 2D quadrature phase alternation sequence provides the phase information in the t_1 domain necessary for the pure absorption representation of the 2D spectrum; i.e., we obtain four quadrant phase information (*7*). $S(\omega_1, \omega_2)$ obtained by the above procedure (known as hypercomplex FT) is not, in general, a 2D absorption spectrum, but an admixture of absorption and dispersion in both ω_1 and ω_2 axes. In order to project out the 2D absorption representation, one would apply phase corrections as described by Eq. [1] to each 1D spectrum obtained upon FT with respect to t_2 at a given t_1. Analogous phase corrections would then be applied to each spectrum obtained upon FT with respect to t_1 at a given ω_2. As already noted, this procedure is difficult in ESR because of the large phase variation across the spectrum in both frequency domains.

To facilitate accurate projection of 2D absorption lineshapes and to suppress certain artifacts that appear in 2D ELDOR spectra, we have applied a linear prediction method developed by Kumaresan and Tufts (*8*) that was introduced to magnetic resonance by Barkhuijsen *et al.* (*9*). In that initial application to magnetic resonance, the emphasis was on obtaining good frequency information in one-dimensional data. Millhauser and Freed (*10*) demonstrated the application of these methods to two-dimensional electron spin-echo (2D ESE) spectroscopy. The 2D ESE method is distinct from COSY and related techniques in that COSY requires irradiation of the entire spectrum (i.e., nonselective pulses), whereas in 2D ESE one irradiates only a narrow region of the spectrum (i.e., selective pulses), recording the maximum ESE signal voltage as the dc field is swept through the spectrum. Real valued linear prediction is applied to the ESE envelope at each field position in the 2D ESE spectrum, facilitating extrapolation of the time series to zero dead time. In this report we demonstrate the use of complex linear prediction in both axes of a 2D ELDOR spectrum. We show how this new application of the general technique, which we call hypercomplex linear prediction, facilitates the projection of 2D absorption lineshapes as well as the rejection of residual axial peaks and much of the noise.

LINEAR PREDICTION FOR 2D CORRELATION SPECTROSCOPY

The basis for (autoregressive) linear prediction is that a discrete time series

$$\{x_1, x_2, \ldots, x_N\} \qquad [3]$$

can be modeled by the expression

$$x_n = \sum_{i=1}^{M} b_i x_{n-i}, \qquad [4]$$

where the set $\{b_i\}$ are called the forward linear prediction (lp) coefficients, and the order M is less than N. The implication of Eq. [4] is that each sampling of the time series can be expressed as a linear combination of the M previous ones. With the application of backward lp, described by writing Eq. [4] in the backward sense, i.e.,

$$x_n = \sum_{i=1}^{M} a_i x_{n+i}, \qquad [5]$$

one can model an FID in terms of exponentially damped sinusoids and determine all of the relevant parameters: frequency, time constant, amplitude, and phase. In such a procedure one first generates a set of coupled equations obtained upon writing Eq. [5] for the $N - M$ possible values of n. The least-squares solution for the set of backward lp coefficients, $\{a_i\}$, in terms of the N complex data points, is written as

$$\begin{bmatrix} x_2 & x_3 & \cdots & x_{M+1} \\ x_3 & x_4 & \cdots & x_{M+2} \\ \vdots & \vdots & \ddots & \vdots \\ x_{N-M+1} & x_{N-M+2} & \cdots & x_N \end{bmatrix} \begin{bmatrix} a_1 \\ a_2 \\ \vdots \\ a_M \end{bmatrix} = \begin{bmatrix} x_1 \\ x_2 \\ \vdots \\ x_{N-M} \end{bmatrix}. \qquad [6]$$

The least-squares problem is solved by determination of the singular values of the data matrix in Eq. [6]. Noise rejection is achieved by subtraction of the root mean

square of the singular values attributed to noise from singular values associated with the FID. There are two parameters which must be selected in order to model the FID: (1) the number of lp coefficients (i.e., the order M) and (2) the number of singular values attributable to signal, which we refer to in the standard fashion as the reduced order, K. Linear prediction yields the frequencies and T_2's, after which a linear least-squares (LS) procedure is used to obtain amplitudes and phases. Once the frequency, T_2, amplitude, and phase of each FID component are known, reconstruction of the FID is facilitated by the expression

$$x'_n \equiv x'(n\Delta t) = \sum_{j=1}^{K} c_j \exp(-n\Delta t/T_{2j})\cos(\omega_j n\Delta t + \phi_j), \qquad [7]$$

representing one quadrature component and an analogous expression for the other quadrature component. As noted above, the phases, ϕ_j, may vary substantially across the spectrum, so that the spectrum obtained upon FT of the reconstructed FID described by Eq. [7] is an admixture of absorption and dispersion. To remedy this problem we zero the K phases, $\{\phi_j, j = 1, K\}$, prior to reconstruction of the FID, so that upon FT of the LPSVD result we obtain the pure absorption lineshapes. This procedure is easily generalized to two frequency dimensions by applying complex LPSVD to each FID prior to FT with respect to t_2, collecting the results of the FT as described by Eq. [2], then applying complex LPSVD once again in the t_1 domain. If the phases, ϕ_j, are zeroed at each call to LPSVD, the pure absorption representation of the 2D spectrum is retrieved.

In addition to projection of pure 2D absorption lineshapes, LPSVD facilitates removal of distortions found in all of our 2D FTESR spectra near $\omega_1 = 0$. The source of these distortions is a combination of extra amplitude modulation in t_1 due to variations in the MW pulse flip angle as a function of t_1 (arising from distortions in the second MW pulse) and incomplete cancellation of axial peaks (*4*). To remove these distortions we reject components whose frequencies fall within a band centered at $\omega_1 = 0$ by excluding them from the reconstructed FID; i.e., we apply a narrow reject filter of desired width (usually ±3 MHz) in ω_1. Careful experimental adjustment of the MW carrier frequency ensures that all three hf lines are off resonance by at least 3 MHz, so that no spectral information is destroyed upon application of the narrow reject filter. Elimination of these distortions improves the accuracy of our measurements of 2D absorption volume integrals, especially for those peaks close in frequency, ω_1, to $\omega_1 = 0$.

The application of LPSVD to 2D ELDOR data is based upon the following theoretical expressions which describe the experiment (*4, 11*). Let $s'(T, t_1, t_2)$ represent the time-domain 2D ELDOR spectral function obtained with three MW pulses of equal phase. Then

$$s'(T, t_1, t_2) = B' \sum_{nml} c'_{nml}\exp(-\Lambda_n t_2)\exp(-T/\tau_m)\mathrm{Re}\left(\sum_j b_{lj}\exp(-\Lambda_j t_1)\right), \qquad [8]$$

where the τ_m represent the decay times associated with magnetization transfer and the c'_{nml} and b_{lj} are the relative amplitudes; the imaginary parts of the Λ_j are the precessional frequencies whereas the real parts represent the homogeneous widths;

i.e., $\Lambda_j = (T_{2,j}^{-1} - i\omega_j)$. Equation [8] shows that the 2D ELDOR spectra are, in the t_1 and t_2 time domains, sums of decaying sinusoids as assumed by LPSVD. In the case of motionally narrowed nitroxides with magnetization transfer driven by Heisenberg spin exchange we can derive from Eq. [8] the simple expression

$$\omega_{HE} = \frac{1}{T} \ln\left(\frac{2a_{mj}V_j + V_m}{V_m - a_{mj}V_j}\right), \qquad [9]$$

where the V_j are determined from volumes of auto peaks (which go as V_j^3) and the a_{mj} are the appropriate ratios of observed cross-peak to auto-peak volumes, and ω_{HE} is the Heisenberg exchange rate. Equation [9] emphasizes the importance of obtaining accurate relative peak volumes from the 2D absorption spectrum.

RESULTS

In our 1D FTESR experiment we record the in-phase and quadrature components of the FID following a $\pi/2$ MW pulse, taking care to cancel image peaks with the four-step CYCLOPS image cancellation sequence (*12*). The spectrum of 2,2,6,6-tetramethyl-4-piperidone-*N*-oxyl-d_{16} (pd-tempone) in toluene-d_8 obtained upon FT of the FID is shown in Fig. 1a (only one of the quadrature components is shown). Superimposed on these data is the spectrum obtained upon FT of the LPSVD-treated FID. The absorption spectrum projected from the LPSVD-treated data is given in Fig. 1b. LPSVD enabled a clear distinction in this example between singular values associated with noise and those associated with the three ^{14}N hf components. The "signal" singular values were at least an order of magnitude greater than the rms of the "noisy" singular values. Weak ^{13}C sidebands present in the data were not recovered by LPSVD because of their smaller amplitudes relative to the noise; some of these components could be recovered by increasing the order M.

In our 2D ELDOR experiments we record the in-phase and quadrature components of the FID during the detection period for each of 16 different phase alternation sequences at 90 different values of t_1. The 16-step phase alternation scheme incorporates 2D quadrature detection as described above, as well as sequences for the cancellation of axial peaks and transverse interference (*4*). The 2D ELDOR spectrum of pd-tempone in toluene-d_8 at 21°C is shown in Fig. 2a; note that this is an absolute value plot (i.e., the square root of the power spectrum). The application of Eq. [9] to the spectrum of Fig. 2a gives the result $\omega_{HE} = 4.89 \times 10^6\ s^{-1}$, where we have compared relative amplitudes, rather than volumes, of cross peaks and auto peaks. Since all three hf lines in the spectrum of Fig. 2a have about the same T_2, we can expect reasonable agreement between ω_{HE} determined from volume integrals and from peak amplitudes as described.

We applied linear prediction to this same data set by using 24 complex lp coefficients in the t_2 domain, and up to 60 coefficients in the t_1 domain. In the t_2 domain six of the singular values were attributed to signal, whereas in the t_1 domain up to 12 were attributed to signal. The required CPU time was approximately 4 h on a Prime 9955 computer, including the time required for FFTs. LPSVD consistently recovered three components in the t_2 domain, corresponding to the three hf lines, and no greater than six components in the t_1 domain. Projection of pure absorption lineshapes was per-

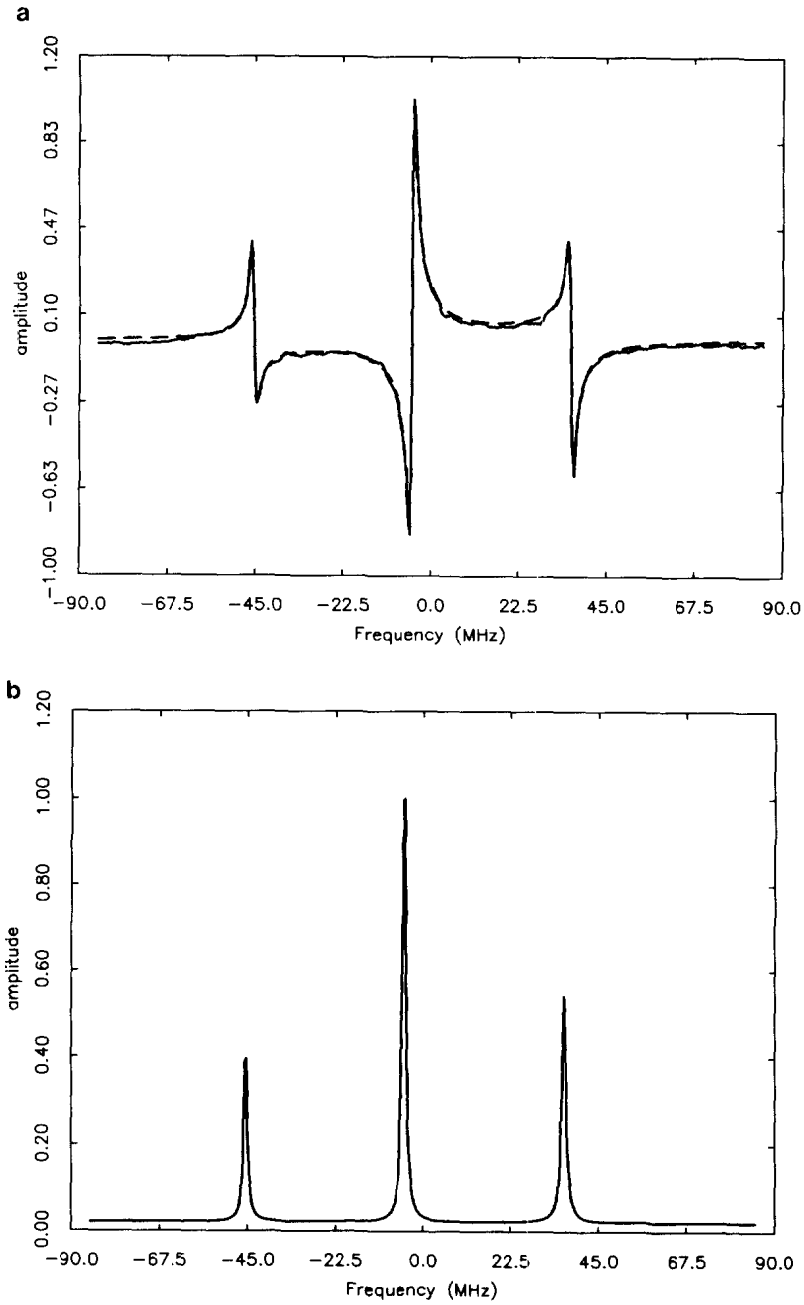

FIG. 1. (a) FT spectrum of 5.1×10^{-4} M pd-tempone in toluene-d_8 at 21°C (solid line) obtained from the average of 40 FIDs, each consisting of 256 complex data points extending to 1.2 μs; FT of the same FID after LPSVD (dashed line) with $M = 20$ and $K = 6$; (b) FT spectrum after LPSVD with projection of pure absorption lineshapes.

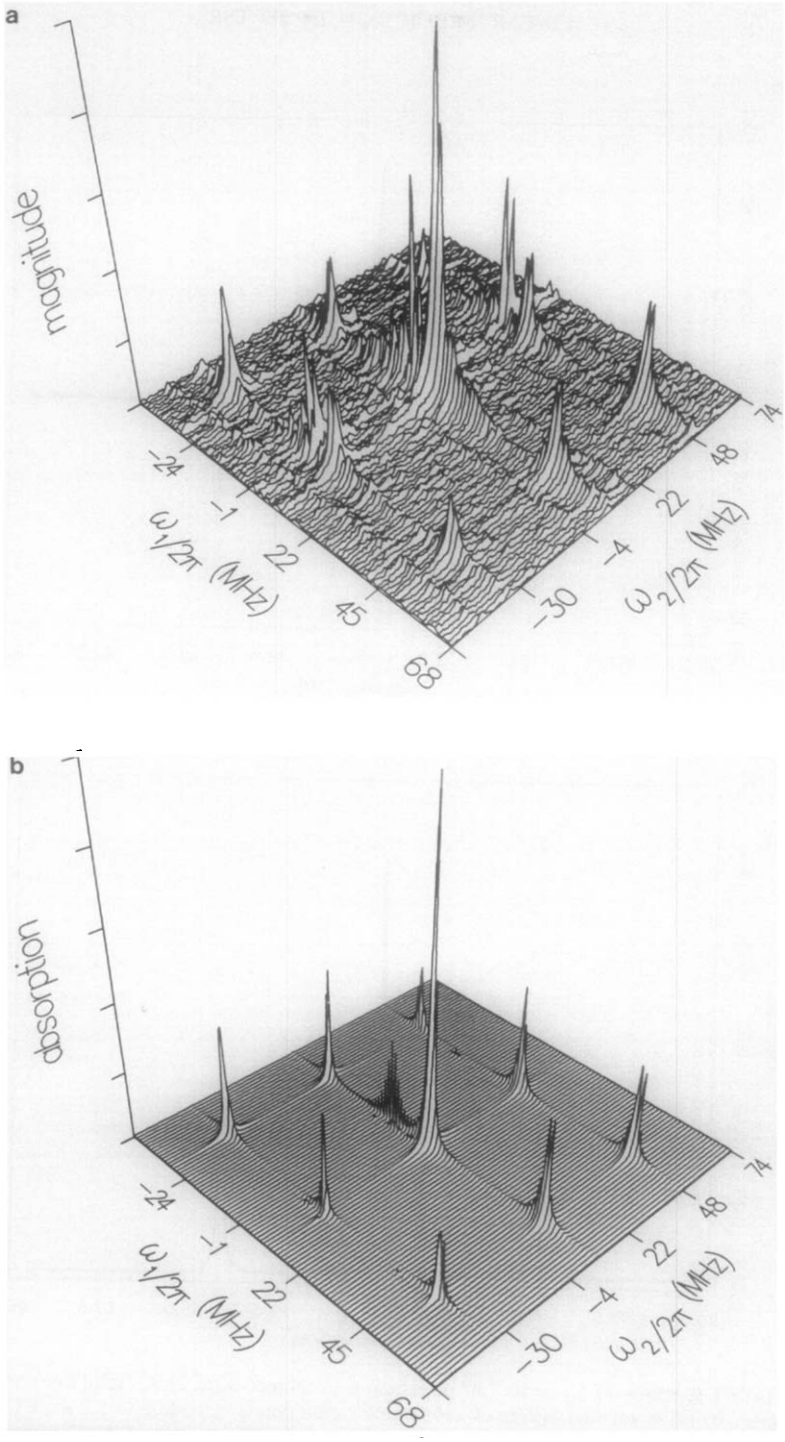

FIG. 2. (a) Absolute value 2D ELDOR spectrum of 1.17×10^{-3} M pd-tempone in toluene-d_8 at 21°C; mixing time $T = 3.10 \times 10^{-7}$ s; 90 t_1 steps; 256 complex data points per FID extending to 1 μs, data from Ref. (*4*). (b) LPSVD-projected pure 2D absorption representation of the same spectrum; $M = 24$, $K = 6$ in the t_1 domain, $M = 60$, $K = 12$ in the t_2 domain; the broad peak near the center of the spectrum (at $\omega_1/2\pi = -8$ MHz) has zero width in ω_2 (hence zero volume) and is apparently an artifact of the computation.

formed in both time domains. Extrapolation of the time series in t_1 to 128 points eliminated artifacts caused by t_1 truncation and enabled a more accurate determination of baseplane offset. In Fig. 2b we illustrate the LPSVD result obtained after eliminating components for which $|\omega_1/2\pi| < 3$ MHz (i.e., narrow reject filtering); note the considerable improvement in signal/noise ratio. The volume integral of each 2D absorption line was measured by numerically integrating in the ω_2 domain and summing the results over the discrete values of ω_1. Estimation of the Heisenberg exchange rate from ratios of volume integrals with the use of Eq. [9] gave the result $\omega_{HE} = 4.59 \times 10^6\ s^{-1}$, in good agreement with the result obtained from Fig. 2a and with the ESE result, $\omega_{HE} = 4.25 \pm 0.60 \times 10^6\ s^{-1}$ (*4*).

DISCUSSION

Many possibilities exist for improvement of the 2D linear prediction method presented in this report. First, we consider potential improvements in the computational method for solving Eq. [6]. The SVD algorithm is generally the most stable method of determining the singular values of the rectangular lp data matrix [call it **A**], but it is also the most computationally inefficient. An alternative approach is to solve for the eigenvalues of the matrix $\mathbf{A}^\dagger\mathbf{A}$, which are simply related to the singular values of **A** (*13*). This method is computationally more efficient than SVD but may become unstable in the case of large order M. Barkhuijsen *et al.* have nevertheless found this technique to be generally successful in LPSVD applications (*9, 14*). Related computational methods for the solution of Eq. [6] and variations on the linear prediction theme have been demonstrated by Tang *et al.* (*15*). We are exploring the use of iterative Lanczos approximation methods for singular value decomposition which are known to predict the large singular values very accurately, and which could be modified to exploit the Hankel structure of **A** (i.e., the property $\mathbf{A}_{ij} = \mathbf{A}_{i+j}$).

We have illustrated that linear prediction may be applied to 2D data simply by applying LPSVD to the constituent 1D spectra (in both t_1 and t_2 time domains). We now propose a substantially different approach, which can truly be considered 2D linear prediction, because it exploits all of the symmetries of 2D COSY type spectra and yields all of the 2D spectral information while performing the analysis entirely in the time domain, i.e., without any Fourier transformation. The procedure, which we will refer to as 2D LPSVD, is carried out as follows: (1) calculate the M lp coefficients in Eq. [6] with the FID obtained at the initial t_1 (for convenience) and determine the frequencies and T_2's; (2) recognizing that frequencies and T_2's are the same for all of the FIDs (i.e. along the t_2 axis) irrespective of the value of t_1, perform the linear LS procedure on each FID to determine amplitudes and phases at each t_1 and for each of the quadrature components in t_1 (i.e., s' and s'', cf. Eq. [2]), utilizing the frequencies and T_2's obtained in step 1; (we now define a time series with parametric dependence on t_1 by the expression

$$x_{nm} \equiv x(n\Delta t_1, m\Delta t_2) = \sum_{j=1}^{K} c_j(n\Delta t_1)\exp(-m\Delta t_2/T_{2j})\cos(\omega_{2j}m\Delta t_2 + \phi_{2j}), \quad [10]$$

which reflects the dependence on t_1 of the complex valued amplitudes, c_j, determined in step 2); (3) recognizing that the $c_j(n\Delta t_1)$ in Eq. [10] are themselves time series of the same form as $x(n\Delta t)$ in Eq. [7] (cf. Eq. [8]), perform LPSVD on the $c_j(n\Delta t_1)$

for every component j (corresponding to the different frequency components in the ω_2 frequency domain); and (4) reconstruct the 2D time-domain data with the expression

$$x_{nm} \equiv x(n\Delta t_1, m\Delta t_2) = \sum_{j=1}^{K_2} \sum_{i=1}^{K_1(j)} c_{ij}\exp(-n\Delta t_1/T_{2,1i})\cos(\omega_{1i}n\Delta t_1 + \phi_{1i}) \times \exp(-m\Delta t_2/T_{2,2j})\cos(\omega_{2j}m\Delta t_2 + \phi_{2j}), \quad [11]$$

which is the 2D LPSVD analog of Eq. [7], where c_{ij}, $T_{2,1i}$, $T_{2,2j}$, ω_{1i}, ω_{2j}, ϕ_{1i}, and ϕ_{2j} are the parameters returned by 2D LPSVD, and K_2 is the reduced order in t_2 with $K_1(j)$ the reduced order in t_1 associated with $c_j(n\Delta t_1)$ (cf. Eq. [10]). Equation [11] represents one quadrant of the hypercomplex data, and analogous expressions may be written for the other three quadrants.

For the spectrum of Fig. 2a, consisting of three resonance lines in the ω_2 domain, only four singular value decompositions (as well as some additional computation, primarily LS) would be necessary for the 2D LPSVD calculation. Since SVD is the primary computational burden in LPSVD, this technique represents a dramatic reduction in CPU time (we estimate 90%) relative to the technique demonstrated in Figs. 1b and 2b. In the general case of a 2D spectrum consisting of n resonance lines in the ω_2 domain, 2D LPSVD would require $n + 1$ SVD calculations.[1] Finally, we note that the techniques presented in this report are equally well suited to spectral analysis of COSY type 2D NMR data.

CONCLUSION

We have demonstrated the application of LPSVD to two-dimensional ESR correlation spectroscopy for the projection of the pure 2D absorption lineshapes as well as for spectral enhancement and narrow reject filtering. The recovery of phase-sensitive 2D information from the raw data and the removal of distortions near $\omega_1 = 0$ improve the accuracy of our 2D techniques and enable better comparison between theory and experiment. We obtained good agreement between the Heisenberg exchange rate obtained from absolute value peak amplitudes and that obtained from volume integrals of LPSVD-projected 2D absorption lineshapes in a 2D ELDOR spectrum of pd-tempone in toluene-d_8. We have outlined a two-dimensional formulation of linear prediction which exploits the special symmetries of 2D correlation spectroscopy, and which dramatically reduces the computational burden of LPSVD in these applications.

ACKNOWLEDGMENT

We thank Mr. Nick Bigelow for contributions to the software.

[1] Note added in proof. We have implemented this algorithm on a Convex C1 super minicomputer, and we find that it successfully yields all of the 2D spectral information outlined above in 63 s of CPU time for 256 × 128 point hypercomplex data with 50 lp coefficients in t_2 and 90 lp coefficients in t_1 while using a vectorized SVD algorithm.

REFERENCES

1. J. GORCESTER AND J. H. FREED, *J. Chem. Phys.* **85,** 5375 (1986).
2. J. GORCESTER, G. L. MILLHAUSER, AND J. H. FREED, *in* "Proceedings, XXIII Congress Ampere on Magnetic Resonance, Rome, 1986" p. 562.
3. J. P. HORNAK AND J. H. FREED, *J. Magn. Reson.* **67,** 501 (1986).
4. J. GORCESTER AND J. H. FREED, *J. Chem. Phys.* **88,** 4678 (1988).
5. See Ref. (*4*), Fig. 4.
6. J. KEELER AND D. NEUHAUS, *J. Magn. Reson.* **63,** 454 (1985).
7. D. J. STATES, R. A. HABERKORN, AND D. J. RUBEN, *J. Magn. Reson.* **48,** 286 (1982).
8. R. KUMARESAN AND D. W. TUFTS, *IEEE Trans.* **ASSP-30,** 833 (1982).
9. H. BARKHUIJSEN, R. DE BEER, W. M. M. J. BOVEE, AND D. VAN ORMONDT, *J. Magn. Reson.* **61,** 465 (1985).
10. G. L. MILLHAUSER AND J. H. FREED, *J. Chem. Phys.* **85,** 63 (1986).
11. G. L. MILLHAUSER, J. GORCESTER, AND J. H. FREED, *in* "Electron Magnetic Resonance of the Solid State" (J. A. Weil, Ed.), p. 571, Can. Chem. Soc. Pub., 1987.
12. D. I. HOULT AND R. E. RICHARDS, *Proc. R. Soc. London, A* **344,** 311 (1975).
13. G. H. GOLUB AND C. F. VAN LOAN, "Matrix Computations," Johns Hopkins Univ. Press, Baltimore, 1983.
14. H. BARKHUIJSEN, R. DE BEER, AND D. VAN ORMONDT, *J. Magn. Reson.* **64,** 343 (1985).
15. (*a*) J. TANG, C. P. LIN, M. K. BOWMAN, AND J. R. NORRIS, *J. Magn. Reson.* **62,** 167 (1985); (*b*) J. TANG AND J. R. NORRIS, *J. Chem. Phys.* **84,** 5210 (1986).